THE JOURNAL OF PHYSICAL CHEMISTRY Letters

Letter

pubs.acs.org/JPCL

Plasmon Length: A Universal Parameter to Describe Size Effects in Gold Nanoparticles

Emilie Ringe,*[,†] Mark R. Langille,[†] Kwonnam Sohn,[‡] Jian Zhang,[†] Jiaxing Huang,[‡] Chad A. Mirkin,[†,‡] Richard P. Van Duyne,[†] and Laurence D. Marks[‡]

[†]Department of Chemistry and [‡]Department of Materials Science and Engineering, Northwestern University, Evanston, Illinois 60208, United States

Supporting Information

ABSTRACT: Localized surface plasmon resonances are central to many sensing and signal transmission applications. Tuning of the plasmon energy and line width through particle size and shape is critical to the design of such devices. To gain quantitative information on the size dependence of plasmonic properties, mainly due to retardation effects, we correlated optical spectra and structures for 500 individual gold particles of five different shapes. We show that the effects of size on the dipolar plasmon frequency and line width are shape-independent when size is described by the plasmon length, the length over which the oscillations take place. This result suggests that edge effects are rather unimportant for dipolar modes in a large size range between 50 and 350 nm. Therefore, in describing the size-dependent plasmonic properties of nanoparticles, one should focus on the distance along which the oscillation occurs rather than its intrinsic shape.

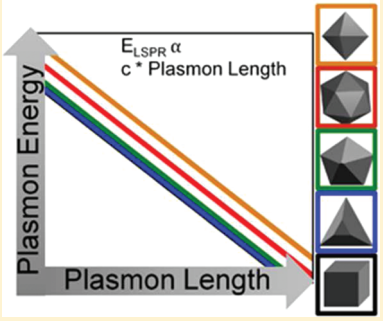

SECTION: Plasmonics, Optical Materials, and Hard Matter

Noble metal nanoparticles are attracting much attention in the scientific community because, unlike bulk metals, their properties can be tuned based upon their shape and size.[1−7] Because such particles can sustain localized surface plasmon resonances (LSPRs), they have been utilized in a variety of promising sensing[3,8,9] and information[10,11] applications. For example, LSPRs enhance the electromagnetic fields around the particle, giving rise to techniques such as surface-enhanced Raman spectroscopy (SERS).[12,13] LSPRs also produce strong, environment-dependent light scattering and absorption, leading to their use as nanoscale refractive index sensors.[3,8,9] The dependence of the plasmon frequency on structural factors is qualitatively known; however, a quantitative understanding of the plasmonic properties of individual particles is limited to a few specific particle shapes and compositions.[5,6,14−17] Here, we show, from an examination of the correlated optical spectra and structures of over 500 individual gold nanoparticles, that the effects of size (mainly due to retardation effects) on the plasmon frequency and line width are shape-independent when the size is described by the plasmon length, the length over which the oscillations take place. The work reported herein suggests that edge effects are rather unimportant for dipolar plasmon modes in a large size range between 50 and 350 nm. Therefore, in describing the size-dependent plasmonic properties of nanoparticles, one should focus on the distance along which the oscillation occurs rather than its intrinsic shape.

Even with the recent advances in the development of shape-controlled syntheses of noble metal nanostructures,[2,18−23] correlated single-particle spectroscopy and electron microscopy has shown to be an invaluable technique that can overcome the difficulties of obtaining quantitative data from the inherently inhomogeneous solution of particles generated from these syntheses. Indeed, single-particle analysis can yield unique information about line widths and precise effects of various structural factors. Early studies on colloidal silver particles[4] paved the road for more recent systematic, statistics-based publications on decahedra,[14] cubes,[6] cages,[15] spheroids,[16] and triangular nanoprisms.[5] Such studies provided important new findings on the effects of size, composition, corner rounding, and surrounding environment on the plasmon energy and, less commonly, on the plasmon lifetime (i.e., peak width). It has been demonstrated that, for instance, the plasmon red shifts and broadens with increasing size due primarily to retardation effects. Simply put, the plasmon resonance frequency changes with particle dimension because the electron oscillation has to accommodate the difference in electromagnetic phase between one end of the particle and the other (i.e., radiative depolarization effects).[24] Note that in the size regime of 50−350 nm, electron surface scattering is not an important contributor to line width.[25] Composition was shown to dictate plasmonic properties because it controls the electrons' polarizability as well as describes losses that are critical for plasmon width.[26] Effects related to substrate composition were also observed.[6]

Received: April 8, 2012
Accepted: May 4, 2012
Published: May 4, 2012

   dx.doi.org/10.1021/jz300426p | J. Phys. Chem. Lett. 2012, 3, 1479−1483

However, a systematic comparison of shapes has not been carried out, despite its critical importance in guiding the choice of particles to be used in a wide range of applications. Thus, to compare the plasmon energy and line width for various Au shapes, cubes, decahedra, icosahedra, octahedra, and truncated bitetrahedra (herein referred to as triangles for simplicity) were synthesized[27−29] and analyzed using correlated single-particle dark field optical microscopy and transmission electron microscopy.[6,30] Representative scattering spectra and electron micrographs of single Au nanoparticles are presented in Figure 1. Each spectrum was fit to one or more Lorentzian line shape

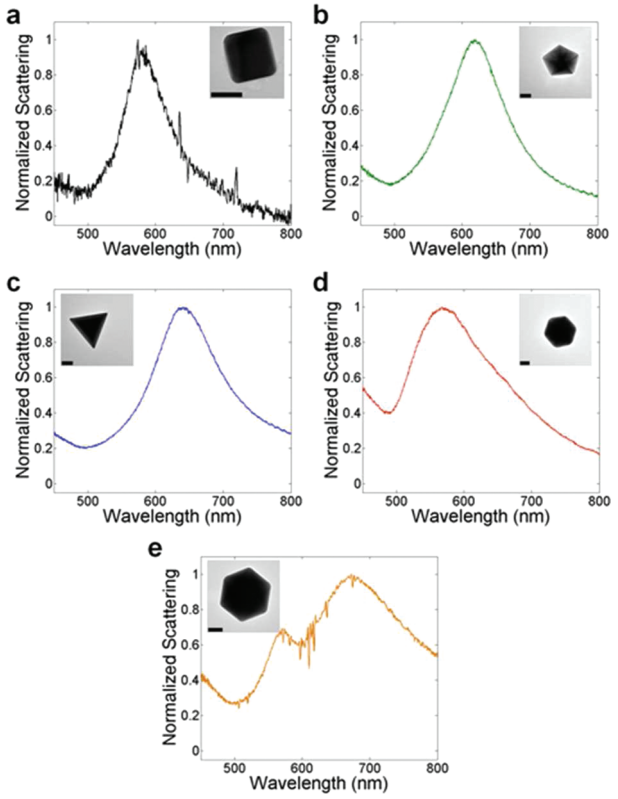

Figure 1. Representative TEM image and associated single-particle LSPR spectrum for Au nanoparicles: (a) cube, (b) decahedron, (c) icosahedron, (d) triangle (truncated bitetrahedron), and (e) octahedron. Scale bars, 50 nm.

functions (one per mode present). The resulting peak positions and line widths of the dipolar resonances (lowest-energy peak) were used for Figure 3; the analysis of covariance is presented below and detailed in the Supporting Information.

Comparing dissimilar structures presents considerable challenges. One difficulty is that the amount of correlated structure−function data required seems prohibitive. The present study overcomes this by using a previously developed high-throughput technique[6,30] to obtain hundreds of correlated single-particle, subnanometer-resolution spectra and electron micrographs. An even more considerable challenge is to compare particles of different shapes but having the same size; not only are such pairs hard to find, they are hard to define. As can be seen in Figure 2a, the traditional way to characterize size for various structures is mostly arbitrary, based on the side length of the repeating triangular or square face. Comparing particles of the same size using this arbitrary side length parameter does not provide much information. As one

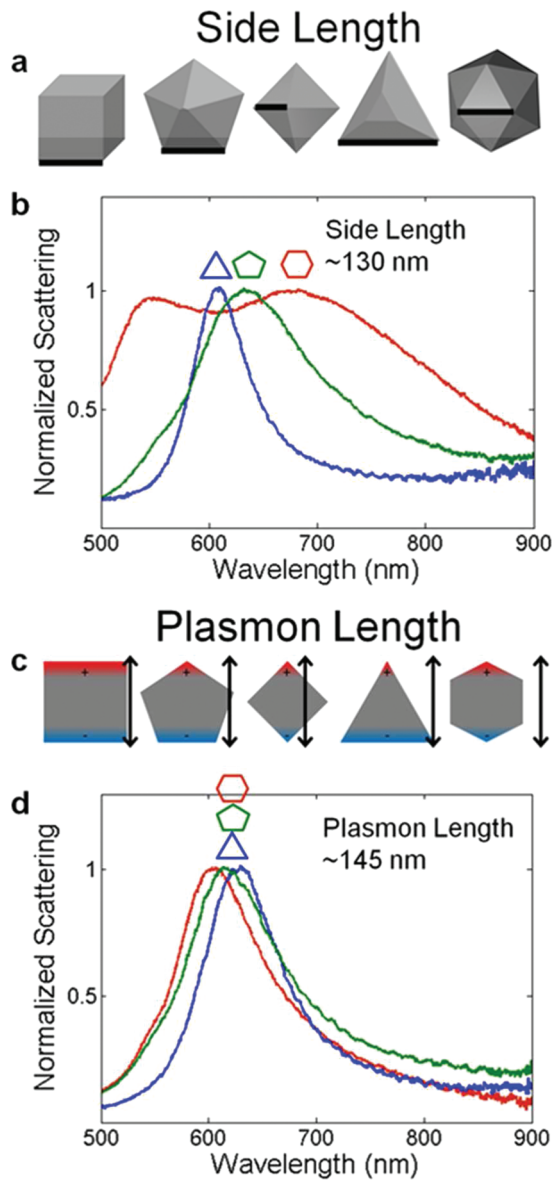

Figure 2. Comparison between the side length and plasmon length as descriptors of nanoparticle size. (a) Definition of the side length for the shapes analyzed. (c) Definition of plasmon length. (b,d) Representative single-particle spectra for Au triangles (blue), decahedra (green), and icosahedra (red) of similar side (b) or plasmon length (d).

might expect, particles of different shapes have different spectra, as illustrated for a truncated bitetrahedron (triangle), decahedron, and icosahedron in Figure 2b. Extracting quantitative values for the size dependence of the plasmon energy and line width provides insight on the behavior of a particular shape, as shown in Figure 3a and c and Supporting Information Table S1. However, the disparity of values for the various shapes seemingly makes this study a case-by-case analysis, where predictive rules will be empirical.

Using arbitrary size parameters thus leads to arbitrary values for the size dependence of plasmonic properties. Another way to approach this issue is to use a size parameter that reflects the plasmon resonance of the particle as the electron oscillation frequency is expected to depend on the separation between charges for a dipolar mode.

dx.doi.org/10.1021/jz300426p | J. Phys. Chem. Lett. 2012, 3, 1479−1483

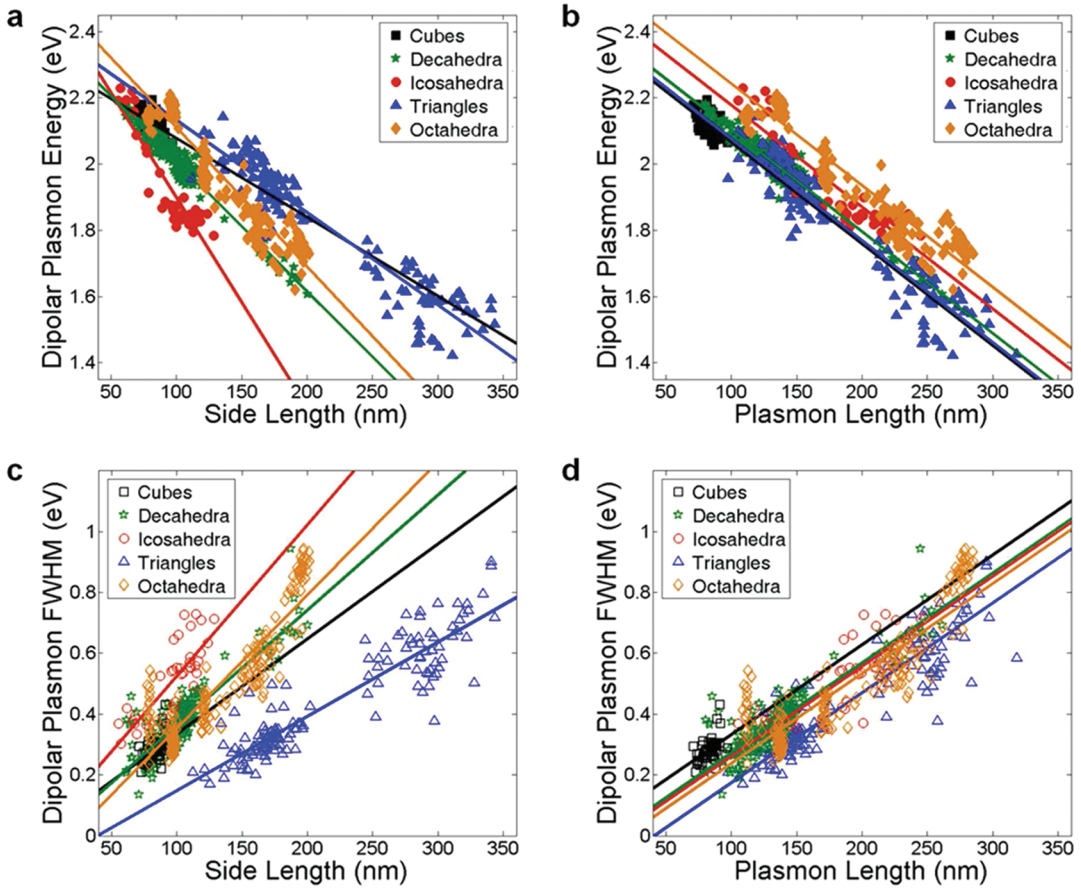

Figure 3. Statistical analysis of size effects using the side and plasmon lengths for Au cubes (black squares), decahedra (green stars), icosahedra (red circles), triangles (blue triangles), and octahedra (orange diamonds). (a) Dipolar plasmon energy dependence on the side length. (b) Dipolar plasmon energy dependence on the plasmon length. (c) Full width at half-maximum (fwhm) dependence on the side length. (d) The fwhm dependence on the plasmon length. Parallel slopes in panels (b) and (d) were obtained from analysis of covariance.

This size parameter is defined for dipolar plasmons as the distance between regions of opposite charge created by the (plasmon) electron oscillation. We will call this physically relevant parameter the "plasmon length"; it is illustrated in Figure 2c. To determine this length for specific shapes, results from numerical calculations and plasmon field mapping experiments were used. The computed vector plots of the induced polarization in octahedra presented by Li et al. clearly show apex to apex oscillation for the dipolar mode.[31] Results from Kelly et al.[1] and Brioude and Pileni[32] supported the plasmon length assignment for triangles, while the findings of McMahon et al.,[30] Sherry et al.,[33] and Ringe et al.[34] were used to determine this parameter for cubes. The plasmon length of decahedra was established based on the computational results of Pastoriza-Santos et al.[35] and Sánchez-Iglesias et al.[36] No information was found on the plasmonic properties of icosahedra as this seems to be the first systematic structure−function analysis for this shape. Its plasmon length was deduced by analogy to octahedral and spherical particles.

Strikingly, particles with different shapes but comparable plasmon lengths have similar LSPR spectra, as can be seen in Figure 2d. Even more notable is the homogeneity in the size dependence of the dipolar plasmon energy and line width for the various shapes studied. As shown in Figure 3b and d and Supporting Information Tables S2−S3, analysis of covariance yields shape-independent values for the slope of the plasmon energy as a function of size (−3.08(4) meV/nm) and for the slope of the plasmon line width as a function of size (2.96(6) meV/nm). This linearity and shape independence can be intuitively understood if one considers that retardation effects are mostly determined by the increase in distance between regions of opposite oscillation-induced charge, with the plasmon length being defined as the distance between such regions. Linear trends for the dipolar plasmon energy variation with size can indeed be extracted from previously published spectra of fixed aspect ratio structures, obtained experimentally for structures such as silver cubes[6] and decahedra,[37] and calculated for silver truncated tetrahedra,[32] for example.

However, despite the identical slopes, there exists a plasmon energy offset between the various shapes studied here, as well as differences between the spectra of particles with similar plasmon lengths. This difference highlights the modest, yet present, effect of shape on plasmonic properties for a particle of a given size, as predicted by Mie−Gans theory[38] (also see Supporting Information) and as observed for cubes and triangles with different corner rounding.[30,39] The findings presented here are indeed consistent with the blue shift expected when moving toward isotropic shape; the plasmon energy for a given size goes as triangles ≈ cubes < decahedra < icosahedra < octahedra, that is, following the general trend expected for highly anisotropic to sphere-like particles.

The concept of plasmon length, an intrinsic property of the nanoparticle, offers the opportunity to predict the plasmon energy and line width dependence on size without having to

dx.doi.org/10.1021/jz300426p | J. Phys. Chem. Lett. 2012, 3, 1479−1483

rely on experiments or detailed calculations; it also provides a powerful framework to compare various shapes, real or hypothetical. This Letter demonstrates and explains how plasmon length describes size effects in Au nanoparticles, yielding shape-independent variations of the plasmon energy and line width. However, this approach is only valid in the cases of particles with fixed aspect ratio and well-formed vertices, with homogeneous small corner rounding for all sizes. For large corner rounding heterogeneities, it might be necessary to include other parameters in order to fully describe simultaneously the size and rounding dependence of plasmon energy and decay. Additionally, shape and size effects have not yet been systematically studied for various Ag shapes. Because of differences in dielectric constants,[40] plasmon resonance frequencies in Ag nanoparticles are expected to have a more acute size dependence than their Au counterparts. Whether size effects are shape-independent in Ag particles remains to be determined.

The complex behavior of nanoparticles makes them valuable for many applications ranging from biosensing[8,9] to surface-enhanced spectroscopies,[12] given that we can understand and predict their optical properties. Plasmon length, an intrinsic and physical way to describe the size of a plasmonic particle, provides a useful framework to explain resonance energy and line width dependence on particle size. Given the extensive recent advances in the ability to deliberately make one-component and two-component structures for Au and Ag,[2,7,18−23,27−29] the plasmon length parameter will become increasingly important in describing plasmonic properties of noble metal nanostructures.

EXPERIMENTAL SECTION

Nanoparticle Synthesis. Poly(diallyldimethylammonium) (PDDA)-capped Au octahedra were synthesized following a previously reported procedure.[29] Poly(vinylpyrrolidone) (PVP)-capped Au decahedra were produced by reduction of hydrogen tetrachloroaurate ($HAuCl_4$) following a previously reported method;[27] icosahedra and triangles were obtained as a reaction byproduct. Cetyltrimethylammoniumbromide (CTAB)-capped Au cubes were synthesized in a seed-mediated process by reducing $HAuCl_4$ with ascorbic acid.[28]

Spectroscopy and Electron Microscopy. An aqueous suspension of particles was deposited and dried on the Formvar (polyvinyl formal, refractive index = 1.5[41]) side of carbon-type B grids (cubes) or ultrathin-type A grids (decahedra, icosahedra, triangles, octahedra) obtained from Ted Pella, Inc. The grids were rinsed with water to remove excess surfactant, yielding a similar dielectric environment for all particles. Dark field scattering, using unpolarized white light, was used to obtain single-particle scattering spectra following a previously reported procedure.[6,30] Spectra of individual nanoparticles were fit to Lorentzian line shape functions to obtain the dipolar peak position and width. Transmission electron microscope (TEM) images providing nanometer-resolution structural information were obtained within 2 days of the optical characterization on a JEOL JEM2100 FAST TEM operated at 200 kV.

ASSOCIATED CONTENT

Supporting Information

Discussion of Mie−Gans theory, additional electron micrographs, and analysis of covariance results. This material is available free of charge via the Internet at http://pubs.acs.org.

AUTHOR INFORMATION

Corresponding Author

*E-mail: emilieringe@u.northwestern.edu.

Notes

The authors declare no competing financial interest.

ACKNOWLEDGMENTS

This work was supported by AFOSR/DARPA Project BAA07-61 (FA9550-08-1-0221), the NSF (CHE0911145), and the NSF MRSEC (DMR-1121262) at the Materials Research Center of Northwestern University. C.A.M. is grateful for support from AFOSR Award FA9550-09-1-0294, DoD/NSSEFF/NPS Award N00244-09-1-0012, Nonequilibrium Energy Research Center (NERC) DOE Award DE-SC0000989, Nanoscale Science and Engineering Initiative NSF Award EEC-0647560, NSF- MRSEC (DMR-0520513 and DMR-1121262), and shared Facilities at the Materials Research Center. Microscopy work was performed in the EPIC facility of the NUANCE Center, which is support by NSF-NSEC, NSF-MRSEC, the Keck Foundation, the State of IL, and NU. Any opinions, findings, and conclusions or recommendations expressed in this publication are those of the authors and do not necessarily reflect the views of the agency sponsors.

REFERENCES

(1) Kelly, K. L.; Coronado, E.; Zhao, L. L.; Schatz, G. C. The Optical Properties of Metal Nanoparticles: The Influence of Size, Shape, and Dielectric Environment. *J. Phys. Chem. B* **2003**, *107*, 668−677.

(2) Jin, R.; Cao, Y. C.; Hao, E.; Métraux, G. S.; Schatz, G. C.; Mirkin, C. A. Controlling Anisotropic Nanoparticle Growth through Plasmon Excitation. *Nature* **2003**, *425*, 487−490.

(3) Lee, K.-S.; El-Sayed, M. A. Gold and Silver Nanoparticles in Sensing and Imaging: Sensitivity of Plasmon Response to Size, Shape, and Metal Composition. *J. Phys. Chem. B* **2006**, *110*, 19220−19225.

(4) Mock, J. J.; Barbic, M.; Smith, D. R.; Schultz, D. A.; Schultz, S. Shape Effects in Plasmon Resonance of Individual Colloidal Silver Nanoparticles. *J. Chem. Phys.* **2002**, *116*, 6755−6759.

(5) Munechika, K.; Smith, J. M.; Chen, Y.; Ginger, D. S. Plasmon Line Widths of Single Silver Nanoprisms as a Function of Particle Size and Plasmon Peak Position. *J. Phys. Chem. C* **2007**, *111*, 18906−18911.

(6) Ringe, E.; McMahon, J. M.; Sohn, K.; Cobley, C. M.; Xia, Y.; Huang, J.; Schatz, G. C.; Marks, L. D.; Van Duyne, R. P. Unraveling the Effects of Size, Composition, and Substrate on the Localized Surface Plasmon Resonance Frequencies of Gold and Silver Nanocubes: A Systematic Single-Particle Approach. *J. Phys. Chem. C* **2010**, *114*, 12511−12516.

(7) Wiley, B. J.; Im, S. H.; Li, Z.-Y.; McLellen, J.; Siekkinen, A.; Xia, Y. Maneuvering the Surface Plasmon Resonance of Silver Nanostructures through Shape-Controlled Synthesis. *J. Phys. Chem. B* **2006**, *110*, 15666−15675.

(8) Mayer, K. M.; Hafner, J. H. Localized Surface Plasmon Resonance Sensors. *Chem. Rev.* **2011**, *111*, 3828−3857.

(9) Anker, J. N.; Hall, W. P.; Lyandres, O.; Shah, N. C.; Zhao, J.; Van Duyne, R. P. Biosensing with Plasmonic Nanosensors. *Nat. Mater.* **2008**, *7*, 442−453.

(10) Dionne, J. A.; Sweatlock, L. A.; Atwater, H. A.; Polman, A. Plasmon Slot Waveguides: Towards Chip-Scale Propagation with Subwavelength-Scale Localization. *Phys. Rev. B* **2006**, *73*, 035407.

(11) Ebbesen, T. W.; Genet, C.; Bozhevolnyi, S. I. Surface Plasmon Circuitry. *Phys. Today* **2008**, *61*, 44−50.

(12) Stiles, P. L.; Dieringer, J. A.; Shah, N. C.; Van Duyne, R. P. Surface-Enhanced Raman Spectroscopy. *Annu. Rev. Anal. Chem.* **2008**, *1*, 601−626.

(13) Chen, C. K.; Heinz, T. F.; Ricard, D.; Shen, Y. R. Surface Enhanced Second Harmonic Generation and Raman Scattering. *Phys. Rev. B* **1983**, *27*, 1965−1978.
(14) Rodríguez-Fernández, J.; Novo, C.; Myroshnychenko, V.; Funston, A. M.; Sánchez-Iglesias, A.; Pastoriza-Santos, I.; Pérez-Juste, J.; García de Abajo, F. J.; Liz-Marzán, L. M.; Mulvaney, P. Spectroscopy, Imaging, and Modeling of Individual Gold Decahedra. *J. Phys. Chem. C* **2009**, *113*, 18623−18631.
(15) Hu, M.; Chen, J.; Marquez, M.; Xia, Y.; Hartland, G. V. Correlated Rayleigh Scattering Spectroscopy and Scanning Electron Microscopy Studies of Au−Ag Bimetallic Nanoboxes and Nanocages. *J. Phys. Chem. C* **2007**, *111*, 12558−12565.
(16) Tcherniak, A.; Ha, J. W.; Dominguez-Medina, S.; Slaughter, L. S.; Link, S. Probing a Century Old Prediction One Plasmonic Particle at a Time. *Nano Lett.* **2010**, *10*, 1398−1404.
(17) Blaber, M. G.; Henry, A.-I.; Bingham, J. M.; Schatz, G. C.; Van Duyne, R. P. LSPR Imaging of Silver Triangular Nanoprisms: Correlating Scattering with Structure Using Electrodynamics for Plasmon Lifetime Analysis. *J. Phys. Chem. C* **2012**, *116*, 393−403.
(18) Zhang, J.; Li, S.; Wu, J.; Schatz, G. C.; Mirkin, C. A. Plasmon-Mediated Synthesis of Silver Triangular Bipyramids. *Angew. Chem., Int. Ed.* **2009**, *48*, 7787−7791.
(19) Jin, R.; Cao, Y.; Mirkin, C. A.; Kelly, K. L.; Schatz, G. C.; Zheng, J. Photo-Induced Conversion of Silver Nanospheres to Nanoprisms. *Science* **2001**, *294*, 1901−1903.
(20) Xia, Y.; Xiong, Y.; Lim, B.; Skrabalak, S. E. Shape-Controlled Synthesis of Metal Nanocrystals: Simple Chemistry Meets Complex Physics? *Angew. Chem., Int. Ed.* **2009**, *48*, 60−103.
(21) Jana, N. R.; Gearheart, L.; Murphy, C. J. Wet Chemical Synthesis of High Aspect Ratio Cylindrical Gold Nanorods. *J. Phys. Chem. B* **2001**, *105*, 4065−4067.
(22) Nikoobakht, B.; El-Sayed, M. A. Preparation and Growth Mechanism of Gold Nanorods (NRs) Using Seed-Mediated Growth Method. *Chem. Mater.* **2003**, *15*, 1957−1962.
(23) Langille, M. R.; Zhang, J.; Mirkin, C. A. Plasmon-Mediated Synthesis of Heterometallic Nanorods and Icosahedra. *Angew. Chem., Int. Ed.* **2011**, *50*, 3543−3547.
(24) Myroshnychenko, V.; Rodríguez-Fernandez, J.; Pastoriza-Santos, I.; Funston, A. M.; Novo, C.; Mulvaney, P.; Liz-Marzán, L. M.; García de Abajo, F. J. Modelling the Optical Response of Gold Nanoparticles. *Chem. Soc. Rev.* **2008**, *37*, 1792−1805.
(25) Hartland, G. V. Optical Studies of Dynamics in Noble Metal Nanostructures. *Chem. Rev.* **2011**, *111*, 3858−3887.
(26) Link, S.; Wang, Z. L.; El-Sayed, M. A. Alloy Formation of Gold−Silver Nanoparticles and the Dependence of the Plasmon Absorption on Their Composition. *J. Phys. Chem. B* **1999**, *103*, 3529−3533.
(27) Seo, D.; Yoo, C. I.; Chung, I. S.; Park, S. M.; Ryu, S.; Song, H. Shape Adjustment between Multiply Twinned and Single-Crystalline Polyhedral Gold Nanocrystals: Decahedra, Icosahedra, and Truncated Tetrahedra. *J. Phys. Chem. C* **2008**, *112*, 2469−2475.
(28) Sohn, K.; Kim, F.; Pradel, K. C.; Wu, J.; Peng, Y.; Zhou, F.; Huang, J. Construction of Evolutionary Tree for Morphological Engineering of Nanoparticles. *ACS Nano* **2009**, *3*, 2191−2198.
(29) Li, C.; Shuford, K. L.; Chen, M.; Lee, E. J.; Cho, S. O. A Facile Polyol Route to Uniform Gold Octahedra with Tailorable Size and Their Optical Properties. *ACS Nano* **2008**, *9*, 1760−1769.
(30) McMahon, J. M.; Wang, Y.; Sherry, L. J.; Van Duyne, R. P.; Marks, L. D.; Gray, S. K.; Schatz, G. C. Correlating the Structure, Optical Spectra, and Electrodynamics of Single Silver Nanocubes. *J. Phys. Chem. C* **2009**, *113*, 2731−2735.
(31) Li, C.; Shuford, K. L.; Chen, M.; Lee, E. J.; Cho, S. O. A Facile Polyol Route to Uniform Gold Octahedra with Tailorable Size and Their Optical Properties. *ACS Nano* **2008**, *2*, 1760−1769.
(32) Brioude, A.; Pileni, M. P. Silver Nanodisks: Optical Properties Study Using the Discrete Dipole Approximation Method. *J. Phys. Chem. B* **2005**, *109*, 23371−23377.
(33) Sherry, L. J.; Chang, S.-H.; Schatz, G. C.; Van Duyne, R. P.; Wiley, B. J.; Xia, Y. Localized Surface Plasmon Resonance Spectroscopy of Single Silver Nanocubes. *Nano Lett.* **2005**, *5*, 2034−2038.
(34) Ringe, E.; Zhang, J.; Langille, M. R.; Sohn, K.; Cobley, C. M.; Au, L.; Xia, Y.; Mirkin, C. A.; Huang, J.; Marks, L. D.; Van Duyne, R. P. Effect of Size, Shape, Composition, and Support Film on Localized Surface Plasmon Resonance Frequency: A Single Particle Approach Applied to Silver Bipyramids and Gold Nanocubes. *Mater. Res. Soc. Symp. Proc.* **2010**, *1208*, O10−02.
(35) Pastoriza-Santos, I.; Sanchéz-Iglesias, A.; García de Abajo, F. J.; Liz-Marzán, L. M. Environmental Optical Sensitivity of Gold Nanodecahedra. *Adv. Funct. Mater.* **2007**, *17*, 1443−1450.
(36) Sánchez-Iglesias, A.; Pastoriza-Santos, I.; Pérez-Juste, J.; Rodríguez-González, B.; Abajo, F. J. G. d.; Liz-Marzán, L. M. Synthesis and Optical Properties of Gold Nanodecahedra with Size Control. *Adv. Mater.* **2006**, *18*, 2529−2534.
(37) Pietrobon, B.; Kitaev, V. Photochemical Synthesis of Monodisperse Size-Controlled Silver Decahedral Nanoparticles and Their Remarkable Optical Properties. *Chem. Mater.* **2008**, *20*, 5186−5190.
(38) Gans, R. Über die Form Ultramikroskopischer Goldteilchen. *Ann. Phys.* **1912**, *342*, 881−900.
(39) Sherry, L. J.; Jin, R.; Mirkin, C. A.; Schatz, G. C.; Van Duyne, R. P. Localized Surface Plasmon Resonance Spectroscopy of Single Silver Triangular Nanoprisms. *Nano Lett.* **2006**, *6*, 2060−2065.
(40) Johnson, P. B.; Christy, R. W. Optical Constants of the Noble Metals. *Phys. Rev. B* **1972**, *6*, 4370−4379.
(41) Shukla, R. P.; Chowdhury, A.; Gupta, P. D. Interferometric Determination of Thickness of Free-Standing Formvar Films. *Opt. Eng.* **1994**, *33*, 1881−1884.